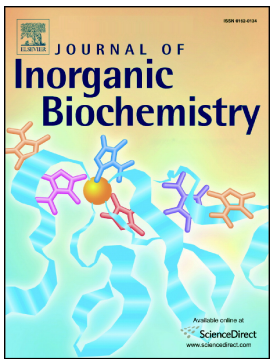

Thiosemicarbazone-metal complexes exhibiting cytotoxicity in colon cancer cell lines through oxidative stress

Raquel Alcaraz, Pilar Muñiz, Mónica Cavia, Óscar Palacios, Katia G. Samper, Rubén Gil-García, Alondra Jiménez-Pérez, Javier García-Tojal, Carlos García-Girón

PII: S0162-0134(19)30491-X

DOI: https://doi.org/10.1016/j.jinorgbio.2020.110993

Reference: JIB 110993

To appear in: *Journal of Inorganic Biochemistry*

Received date: 25 July 2019

Revised date: 3 January 2020

Accepted date: 5 January 2020

Please cite this article as: R. Alcaraz, P. Muñiz, M. Cavia, et al., Thiosemicarbazone-metal complexes exhibiting cytotoxicity in colon cancer cell lines through oxidative stress, *Journal of Inorganic Biochemistry* (2020), https://doi.org/10.1016/j.jinorgbio.2020.110993

Thiosemicarbazone-metal complexes exhibiting cytotoxicity in colon cancer cell lines through oxidative stress

Raquel Alcaraz[a*], Pilar Muñiz[b*], Mónica Cavia[b], Óscar Palacios[c], Katia G. Samper[c], Rubén Gil-García[d], Alondra Jiménez-Pérez [d], Javier García-Tojal[d], Carlos García-Girón[e]

a. Unidad de Investigación. Hospital Universitario de Burgos. Avd Islas Baleares, 3, 09006 Burgos, Spain.

b. Departamento de Biotecnología y Ciencia de los Alimentos. Universidad de Burgos Plaza Misael Bañuelos s/n, 09001 Burgos, Spain.

c. Departament de Química, Universitat Autònoma de Barcelona, E-08193 Cerdanyola del Vallès, Barcelona, Spain.

d. Departamento de Química. Universidad de Burgos, 09001 Burgos, Spain.

e. Servicio de Oncología Médica. Hospital Universitario de Burgos. Avd Islas Baleares, 3, 09006 Burgos, Spain.

* Corresponding author: +34 947 281964;
e-mail address: ralcaraz@hubu.es; pmuniz@ubu.es

To the memory of Prof. Juan Manuel Salas

***Keywords*:** Cell Death. Cobalt compounds. Colon carcinoma. Iron compounds. Oxidative stress. Thiosemicarbazone.

Abstract

Colorectal cancer is the third most common type of cancer and has a high incidence in developed countries. At present, specific treatments are being required to allow individualized therapy depending on the molecular alteration on which the drug may act. The aim of this project is to evaluate whether HPTSC and HPTSC* thiosemicarbazones (HPTSC = pyridine-2-carbaldehyde thiosemicarbazone and HPTSC* = pyridine-2-carbaldehyde 4N-methylthiosemicarbazone), and their complexes with different transition metal ions as Cu(II), Fe(III) and Co(III), have antitumor activity in colon cancer cells (HT-29 and SW-480), that have different oncogenic characteristics. Cytotoxicity was evaluated and the involvement of oxidative stress in its mechanism of action was analyzed by quantifying the superoxide dismutase activity, redox state by quantification of the thioredoxin levels and reduced/oxidized glutathione rate and biomolecules damage. The apoptotic effect was evaluated by measurements of the levels of caspase 9 and 3 and the index of histones. All the metal-thiosemicarbazones have antitumor activity mediated by oxidative stress. The HPTSC*-Cu was the compound that showed the best antitumor and apoptotic characteristics for the cell line SW480, that is *KRAS* gene mutated.

1.-Introduction

Colorectal cancer (CRC) is the third most common malignant neoplasm and the fourth main cause of cancer death in the world, with nearly 1.8 million new cases and 881,000 deaths in 2018 [1]. The *KRAS* gene is a major oncogenic driver of CRC [2, 3] and oncogenic activation of *KRAS* is mutually exclusive and occurs in approximately 40% of all CRCs [4]. These mutations play distinct roles in development and therapy resistance of CRC [5]. The high variability of response and results in patients with CRC treated with the common treatments has highlighted the need to identify new drugs that allow more individualized treatments [6].

Cancer cells have increased reactive oxygen species (ROS) levels compared to normal cells [7]. This phenomenon is associated with oncogenic transformations and renders them more susceptible to harmful effects of the increased oxidative stress induced by treatment with drugs. The increase of the oxidative stress and disruption of redox homeostasis of tumor cells appears to be an attractive and promising approach for cancer therapy. The ability of cancer cells to operate under substantially higher levels of oxidative stress has been demonstrated with increased levels of thioredoxin (TRX) and malondialdehyde (MDA) in CRC patients [8]. The reduced/oxidized glutathione rate (GSH/GSSG) and the thioredoxin systems are the main controllers of the cytoplasmic redox state and regulate the activity of the different intracellular proteins and transcription factors that bind to DNA and regulate cell growth. *RAS*'s mutated phenotypes in CRC involve an increase in the expression of superoxide radical-generating enzymes [9]. This increase in enzyme expression, by *KRAS* and *EGFR* (Epidermal Growth Factor Receptor) genes, is known to occur through the metabolic pathway MEK-ERK (serine/ tyrosine/ threonine kinase-extracellular signal regulated kinase cascade phosphorylation, resulting in high production of superoxide anion,

which modifies the cell redox state [10]. However, cancer cells are also more susceptible to an increase in oxidative stress through a drug pro-oxidant intervention that augments ROS levels [7].

An emerging target in anticancer oxidative therapy is intracellular generation of ROS via thiosemicarbazone (TSC) chelators of transition metals. TSCs are organic sulfur- and nitrogen-containing compounds whose coordinating ability as chelate ligands has led to their use for the synthesis of a wide range of complexes with different metallic elements, such as copper, iron, cobalt, zinc, etc [11, 12] .The properties of TSCs and their metal complexes have demonstrated their adaptability to a range of applications, making them attractive molecules for further evaluation as novel potential therapeutic agents aimed at cancer treatment [13-18]. Many studies have demonstrated that even slight structural modifications may result in dramatic changes in metal-TSC complex stability, redox potentials, membrane permeability and in vitro biological activities, i.e. antiproliferative activity, induction of apoptosis in cancer cell lines, and specific target inhibition [10]. Among the consolidated results, the literature reports that the presence of a metal ion often increases the activity or contributes to mitigate the side effects of the free ligands [19] and that the putative targets are ribonucleotide reductase [20, 21], topoisomerase IIa [22, 23] and a multidrug resistance protein (MDR1) [24-26], apart from nucleic acids and nucleotides [27-29]. Therefore, a possible emerging target in anticancer oxidative therapy is intracellular generation of ROS via metal chelators [30-33]. Their biological activities can be modified or enhanced by the linkage to essential metal ions such as Fe(III), Cu(II) and Zn(II) [34, 35].

It is well established that α-N-heterocyclic TSCs show the highest antitumor activity among all the TSC compounds studied up to date [36, 37]. In the present work, we have chosen one of the simplest member of the α-N-heterocyclic TSC family, the pyridine-2-

carbaldehyde thiosemicarbazone (HPTSC, see Scheme 1), to perform a research about the influence of the substitution and the coordination to metal ions in the biological activity. This ligand is quite relevant because it represents the moiety common to all the TSC compounds tested as antitumor in clinical trials. In the same way, we have checked the influence of one of the simplest case of substitution, the methylation of the terminal amino group to give pyridine-2-carbaldehyde 4N-methylthiosemicarbazone (HPTSC*). We have selected essential metal elements, as Fe, Co and Cu, to build the coordination compounds. The influence of the TSC substitution and coordination to metal ions on the biological activity of similar TSC systems has been discussed for a long time. In some cases, the substitution of the terminal NH_2 group of the TSC and the coordination to Fe(III) or Cu(II) ions enhance the antiproliferative activity of TSCs [38-45]. However, this trend is not usually observed in Co(III) analogues [46]. This fact is related, at least in part, with the production of ROS. However, in the case of the drug Triapine ®, 3-aminopyridine-2-carbaldehyde TSC, the effect of the entry of a methyl on the terminal amino group does not lead to an increase of the antiproliferative activity [47]. Regarding the metal ions, the addition of Cu(II) inactivates Triapine ®, while potentiates Dp44mT, di-2-pyridilketone 4,4-dimethylthiosemicarbazone [48].

In a previous article, we have studied the biological activities of the HPTSC, HPTSC*, Cu(PTSC)(NO_3) and Cu(PTSC*)(NO_3) compounds [49], where $PTSC^-$ and $PTSC^{*-}$ are the deprotonated forms of HPTSC and HPTSC* after the loss of the H^+ on the hydrazinic nitrogen atom (see Scheme 1). The Cu(II) complexes showed higher cytotoxicity than the free ligands against HT-29 and SW-480 colon carcinoma cell lines, elevated levels of ROS, oxidation of protein and a decrease in the GSH levels.

In the current study, we explore the redox potency and mechanism of action of the same TSC ligands linked to Fe(III) and Co(III) metal ions, and the influence on viability of

colon cancer cells. The tested compounds are $Fe(PTSC)_2(NO_3)(H_2O)$, $Co(PTSC)_2(NO_3)$, $Fe(PTSC^*)_2(NO_3)(H_2O)_3$ and $Co(PTSC^*)_2(NO_3)(H_2O)_3$, whose labels will be HPTSC-Fe, HPTSC-Co, HPTSC*-Fe and HPTSC*-Co, respectively.

Our premise is that an increase in oxidative stress within cancer cells using different TSCs and metals can induce oxidative stress at different points in the oxidative cell cascade and it will provoke an increase in the cytotoxicity resulting in cell death of cancer cells.

2.-Experimental Section

2.1. Synthesis of the thiosemicarbazone compounds

Reactants and solvents employed were purchased from commercial sources and used as received. The synthesis and characterization of the HPTSC and HPTSC* ligands, and the $Cu(PTSC)(NO_3)$ (in this work, HPTSC-Cu), $Cu(PTSC^*)(NO_3)$ (here, HPTSC*-Cu), $Fe(PTSC)_2(NO_3)(H_2O)$ and $Co(PTSC)_2(NO_3)$ complexes have been previously reported [49, 50], and follow published methods [32, 50-56]. Compounds $Fe(PTSC^*)_2(NO_3)(H_2O)_3$ and $Co(PTSC^*)_2(NO_3)(H_2O)_3$ were synthesized as the HPTSC analogous derivatives, from aqueous solutions of the corresponding nitrates and HPTSC* in (1:2) ratio, after addition of diluted NaOH to reach pH 2−5. Yields and characterization details for both complexes are given below, see also Figures S1−S6. Complexes were dissolved in dimethyl sulfoxide (DMSO) (Sigma-Aldrich) to be applied to cell cultures.

$Fe(PTSC^*)_2(NO_3)(H_2O)_3$. Yield: 33 %, 0.187 g. Anal. found: C, 34.35; H, 4.11; N, 22.17; S, 11.61. Calc. for $C_{16}H_{24}FeN_9O_6S_2$ (558.39 g/mol): C, 34.42; H, 4.33; N, 22.58; S, 11.48. Selected IR bands [cm^{-1}, Attenuated Total Reflectance (ATR)]: 3350(b,sh), 3214(m), 1640(w), 1602(w), 1575(s), 1557(vs), 1503(s), 1465(s), 1435 (m), 1388(sh)–$\upsilon_3(NO_3^-)$, 1352 (vs)–$\upsilon_3(NO_3^-$, 1304(vs), 1284(vs), 1254(s), 1230(s), 1171(s), 1153(s),

1116(s), 1098(s), 1035(s), 890(m), 864(w), 826(w)–$\upsilon_2(NO_3^-)$, 765(s), 748(vw,sh), 742(w), 692(w), 651(vw), 623(vw), 602(w), 517(w), 502(w,sh), 447(w), 426(w). Fast Atom Bombardment Mass Spectrometry (FAB^+) mass spectrometry (m/z): 441.93 $[Fe(PTSC^*)_2]^+$, 248.93 $[Fe(PTSC^*)]^+$. UV-vis [Phosphate Buffer Solution (PBS)] at room temperature (RT), (λ_{max}/nm): 204, 241, 304, 354, 445 sh, 597, 825. X-band Electron Paramagnetic Resonance (EPR) signals: powder at RT, $g_{\|}$ = 2.011, $g_{\perp}$ = 2.156; 3.2 x 10^{-4} M solution in a (2: 1, ethylene glycol: PBS) mixture at 120 K, g_1 = 2.182, g_2 = 2.136, g_3 = 2.001; 10^{-3} M solution in DMSO at 120 K, g_1 = 2.183, g_2 = 2.136, g_3 = 2.000.

$Co(PTSC^*)_2(NO_3)(H_2O)_3$. Yield: 34 %, 0.191 g. Anal. found: C, 34.41; H, 4.25; N, 22.48; S, 11.15. Calc. for $C_{16}H_{24}CoN_9O_6S_2$ (561.48 g/mol): C, 34.23; H, 4.31; N, 22.45; S, 11.42. Selected IR bands (cm^{-1}, ATR): ≈3450 (vb,sh), 3220(m), 1643(w), 1602(w), 1578(s), 1560(vs), 1504(s), 1475(s), 1463(s), 1437(m), 1389(sh)–$\upsilon_3(NO_3^-)$, 1347 (vs)–$\upsilon_3(NO_3^-$, 1303(vs), 1280(vs), 1254(s), 1229s), 1173(s), 1154(s), 1119(s), 1100(s), 1036(s), 888(m), 851(vw), 827(w)–$\upsilon_2(NO_3^-)$, 763(m), 740(vw), 742(w), 690(w), 651(vw), 624(vw), 606(w), 514(w), 502(w,sh), 450(w), 420(w). FAB^+ mass spectrometry (m/z): 444.97 $[Co(PTSC^*)_2]^+$, 251.96 $[Co(PTSC^*)]^+$. UV-vis (PBS) at RT, (λ_{max}/nm): 224, 293, 359, 415 sh.

2.2. Cell Culture and treatment

The human colorectal cancer lines HT-29 and SW-480 were purchased from American Type Culture Collection (ATCC). Cells were grown in Dulbecco´s modified Eagle´s medium (DMEM) (Sigma-Aldrich) supplemented with 10% Fetal Bovine Serum (FBS) (Sigma-Aldrich), 1% L-glutamine (Sigma-Aldrich) and 1% Penicillim-Streptomicyn (Sigma-Aldrich) at 37 ºC and 5% CO_2. Cells were detached when were at 80-90% of confluence and 2 x 10^6 subcultures were made in 25 cm^2 cell culture flask. After 24 h of

treatment with the IC50 of the different metal complexes the cells were removed and washed with PBS for clearing the remains of medium. Cells were sonicated and saved al -80 ºC until the determinations were made.

To study the cytotoxicity of the compounds in normal tissue, we reproduced the cell viability assay in the cell line CCD-112, which is colonic fibroblast. The cell line was purchased from the ATCC. Cells were grown in Modified Eagle´s Medium (MEM) (Sigma-Aldrich) supplemented with 10% FBS (Sigma-Aldrich), 1% L-glutamine (Sigma-Aldrich) and 1% Penicillim-Streptomicyn (Sigma-Aldrich) at 37ºC and 5% CO_2. Cells were detached when were at 80-90% of confluence.

2.3. Cell viability assessment MTT

To determine the death activity of the compounds was applied the MTT [3-(4,5-dimethylthiazol-2-yl)-2,5-diphenyltetrazolium bromide] assay. This probe is a colorimetric assay for assessing cell metabolic activity. NADH-dependent cellular oxidoreductase enzymes under defined conditions reflect the number of viable cells present. These enzymes are capable of reducing the tetrazolium dye MTT to its insoluble formazan, which has a purple color.

Briefly, cells were seeded in 96-well multiplates (1.0×10^4 cells/well filled with 200 µL of medium) for 24 h and then exposed for other 24 h to different concentrations of the treatments (2−50 µM of medium of each treatment HPTSC, HPTSC*, and their combinations with metals) or just DMEM/ MEM for the not treated cells (NT). Then, MTT reagent dissolved in PBS was added to the wells at a final concentration of 0.5 mg/mL of DMEM/ MEM and the plate was maintained in the incubator for 2 h at 37 ºC and 5% CO_2. The mitochondrial reductase present in living cells reduces MTT to purple formazan. After incubation, the medium was removed and 200 µL DMSO were added to each well. The absorbance of purple formazan at 570 nm was measured in a

microplate spectrophotometer (MultiSkan, Thermofisher). The experiments were repeated three times in four parallel wells. The viability of treated cells was calculated with respect to the NT cells and the concentration of each treatment that inhibited 50% of cell viability (IC50) was determined, expressing the IC50 values for each fraction in μM.

Assays with oxaliplatin were conducted under the same conditions as assays with TSCs. The drug was diluted in the respective medium to be administered in the three cell lines HT-29, SW-480 and CCD-112. Oxaliplatin concentration range tested was from 0 to 150 μM.

2.4. Superoxide Dismutase (SOD) activity

The total SOD activity was assessed by the method developed by McCord and Fridovich (1969) [57], based on the production of superoxide radicals during the conversion of xanthine (Sigma-Aldrich) to uric acid by xanthine oxidase (Roche), and the inhibition of cytochrome c (Sigma-Aldrich) reduction. Briefly, 20 μl of cellular suspension were added to 125 μL of xanthine, 25 μL of cytochrome C 0.3 mM, 40 U of xanthine oxidase and potassium-phosphate buffer 50 mM-EDTA 0.1 mM pH 7.8, until a final volume of 700 μL. The kinetic of the mixture was measure during 2 min at 546 nm in a spectrophotometer (Shimazu). One unit of SOD activity was defined as the amount of SOD that produces 50% inhibition of cytochrome c reduction.

2.5. Thioredoxin (TRX) and thioredoxin reductase (TRXr) assay

TRX was determined with an ELISA (Enzyme-Linked ImmunoSorbent Assay) kit (WAKO 306-34121). Briefly, 200 μL of the cellular suspension was incubated with anti-TRX antibody for 2 h, and then, the wells were washed to incubate with the conjugate solution for another 2 h and incubated with the substrate solution. The plate

was measure at 450 and 620 nm. The results were calculated from calibration curves and expressed as TRX concentration (μM).

TRXr was measured with a modified method develop by Holmgren and Bjornstedt [58]. The procedure is based on catalysis carried out by the thioredoxin system, which reduces the insulin disulfide group. Briefly, 8 μl of the cell suspension were mixed with, 28 μl water milliQ, and 20 μL of Reagent A (200 μL HEPES [4-(2-hydroxyethyl)-1-piperazineethanesulfonic acid] 1 M, pH 7.6, 40 μL of EDTA 0.2 M, 40 μL of NADPH 40 mg/mL and 500 μL of insulin 10 mg/mL). Then it was added 5 μL of a 60 μM solution of *E. coli* thioredoxin and incubated for 20 min at 37 ºC. Next was added 250 μL of 0.4 mg/mL DTNB (5,5′-dithio-bis-2-nitrobenzoic acid) and 6 M guanidine in Tris-HCl 0.2 M, pH 8, absorbance was determined at 412 nm. The results were calculated from calibration curves e and expressed as TRXr activity (mU/mg protein).

2.6. Reduced/oxidized glutathione (GSH/GSSG) ratio analysis

Aliquots of the cell suspensions collected after the treatment period were immediately acidified with $HClO_4$ (2% final concentration), centrifuged (8000 rpm, 5 min, 4 °C), and the supernatants were frozen at −80 °C until their use as samples. GSH and GSSG levels in these samples were determined using the reaction between the sulfhydryl group of the GSH and DTNB. The GSTNB [mixture between GSH and TNB (2-nitro-5-thiobenzoate)] formed is reduced by glutathione reductase to recycle GSH and produce more TNB. The rate of TNB produced is directly proportional to the recycling reaction, and is directly proportional to the concentration of GSH in the sample. The measurement of TNB absorbance at 410 nm provides an accurate estimate of the GSH content in the sample. Briefly, 75 μL of the cellular suspension was neutralized with triethanolamine 4 M and derivatized with vinylpyridine for 1 h. Then 10 μL of the mixture were incubated with 190 μL of the master mix, which contained NAPDH,

DTNB and glutathione reductase. The kinetic of the enzyme was followed up during 20 min with a plate spectrophotometer (MultiSkan, Thermoficher).

2.7. Carbonyl groups (CGs).

Protein damage was measured by the formation of CGs using the spectrophotometric method described by Levine et al. [59]. Briefly, 150 µL of the cellular suspension was incubated with 500 µL of 10 mM DNPH (2,4-Dinitrophenylhydrazine**)** / 2 M HCl. for 1 h at RT. Protein precipitation was performed using 500 µL of 20% (w/v) of trichloroacetic acid, washing twice with ethanol/ethyl acetate (1:1 v/ v), and samples were centrifuged at 6000 g for 3 min. Finally, 1 mL of 6 M guanidine, pH 2.3, was added and the samples were incubated in a 37 °C for 30 min. CGs was calculated by spectrophotometry at 373 nm, using a molar absorption coefficient of 22,000 M^{-1} cm^{-1}. The CGs levels were then normalized by the protein content of each cell homogenate, expressing the final results as nmol CGs/mg of protein.

2.8. Malondialdehyde (MDA)

Lipid peroxidation was estimated quantifying the MDA levels according to the method described by Grotto et al [60]. Briefly, a volume of 150 µL of sonicated cells were mixed with NaOH and milliQ water for 30 min at 60 ºC was added to 25 µL of Milli-Q water and 25 µL of 3 M NaOH and incubated at 60º C for 30 min in a shaking water bath system. After this, 125 µL of 6% (v/v) H_3PO_4 and 125 µL of 0.8% (w/v) TBA (2-Thiobarbituric acid) were added and the mixture was heated at 90 ºC for 45 min. Then, the mixture was cooled and extracted with 300 µL of n-butanol by vortex-mixing for 1 min and centrifugation at 3,000 g for 10 min. The butanol layer was collected and a volume of 20 µL was injected into a Waters Alliance 2695 Series HPLC (Waters Corporation) equipped with a diode array detector. The column was a Waters SymmetryShield RP18 5 µm 4.6 x 250 mm. The mobile phase was potassium phosphate buffer 50 mM with 35% of methanol with a flow of 1 ml/min. Concentrations of MDA

were calculated from calibration curves obtained using 1,1,3,3-tetramethoxypropane as standard and the results were finally expressed as μM MDA.

2.9. Evaluation of 8OH-2dG/2dG

Suspensions of 5 x 10^6 cells HT-29 and SW-480 will have their DNA extracted using the DNA Maxi Kit from Quiagen. It was enzymatically hydrolysed (DNAase I, phosphodiesterase II and alkaline phosphatase). The mixture of enzymes and DNA was incubated at 37 °C for 6 h. After this time, 250 μL of cold ethanol was added to the product and kept the mixture at −20 ºC for 30 min. The samples were then centrifuged at 15000 g for 30 min. The supernatant was dried and dissolved in 100 μL of ultrapure water. Before pricking, 50 μL of the reconstituted supernatant was mixed with 50 μL of MiliQ water.

Then, 15 μL of the mixture was placed in a HPLC-MS/MS (Agilent triple quadrupole 6460) with a column Zorbax Eclipse XDB-C8 (4.6 x 150mm) 5 μm particle size. The mobile phase was a gradient of MiliQ water (A) and acetonitrile (B) both buffered with 0.1% formic acid. At initial time there was an A concentration of 100%, 3.5 min later he concentration was 60% A and 40% B to end at minute 8 with a 100% B concentration. The flow rate was 0.4 mL/min all the time. The sample was ionized with an electrospray jet stream source. The Sheath Gas Temperature and the Gas Temperature was 300ºC. The flow rate of the Sheath Gas was 11 L/min and the flow rate of the Gas was 3 L/min. The nebulizer was at 30 psi. The method used for the quantification was a standard addition. Each sample was added three different standards (2dG: 1, 10, 20 ppb; 8dG: 0.1, 1, 2 ppb). The transitions with the highest signal (2dG: 152; 8 dG: 168) were those used for quantification and were reinforced by the next two transitions (2dG: 135, 110; 8dG: 140, 112) with the highest signal. The results were calculated with the Mass Hunter quantification software (Agilent Quantitative Analysis version B.07.01). The

product collected after the reactions had to be between the limits with a 10% of deviation to be a correct concentration. The results were expressed as ratio 8OH-2dG/2dG.

2.10. Evaluation of Caspase and Caspase 9

ELISA kits measured these parameters Caspase 3 (Cusabio CSB-E08856h) and Caspasa 9 (Cusabio CSB-E08862h). The protocol of each kit was followed. Briefly, 100 µL of the cellular suspension were incubated for 2 h at 37 ºC with the primary antibody. Next, 100 µL of a biotin secondary antibody was added and incubated for 1 h at 37ºC. After, the wells were washed and HRP-avidin (horseradish peroxidase-avidin) was added and incubated 30 min at 37 ºC. Then, the substrate of the reaction was added and measure at 450 nm in a microplate spectrophotometer (MultiSkan, Thermofisher). The results were expressed as concentration of caspase (µM).

2.11. Cell Death Detection

Cell Death was confirmed by a photometric enzyme immunoassay (Sigma Cat. No 11920685001). This allows the specific determination of mono and oligonucleosomes in the cytoplasmic fraction of cell lysates. The samples were placed into a streptavidin-coated microplate and incubated with a mixture of anti-histone-biotin and anti-DNA-peroxidase. During the incubation, nucleosomes were captured via their histone component by the anti-histone-biotin antibody while binding to the streptavidin-coated microplate. Simultaneously, anti-DNA-peroxidase binds to the DNA part of the nucleosomes.

2.12. Mass spectrometry measurements

The complexes were dissolved in DMSO for FAB^+ Spectrometry measurements, using a *m*-nitrobenzyl alcohol (NBA) matrix. Regarding the Electrospray Ionization (ESI) Mass Spectrometry experiments on the interaction with cytochrome c and myoglobin, stock

aqueous solutions of lyophilized commercial proteins (Sigma-Aldrich) and stock DMSO solutions of the TSCs derivatives were used. Protein: compound (1:5) ratio solutions in NH_4HCO_3 buffer (25 mM, pH 7.0) were incubated for 24 h at 37 ºC. An Electrospray Ionization-Time Of Flight-Mass Spectrometry (ESI-TOF-MS) spectrometer with a HPLC pump coupled at pH 7.0 buffered (20 mM ammonium acetate) was used, with 4500 V and 100 ºC experimental conditions.

2.13. Physical Measurements.

Measurements of pH were made using a CRISON micropH 2002 instrument. Microanalyses were performed with a LECO CHNS-932 analyzer. FAB^+ and ESI mass spectrometry data were obtained on a Micromass AutoSpec and a Bruker Esquire 3000 Plus LC-MAS, respectively. Fourier Transform Infrared Spectroscopy (FT-IR) measurements were carried out in a JASCO FT-IR 4200 spectrometer equipped with an ATR PRO ONE single reflection accessory for ATR measurements. The intensities of reported IR bands are defined as vs = very strong, s = strong, m = medium and w = weak, while b means a broad band and sh is a shoulder. UV-vis spectra were recorded in the 200−1100 nm spectral range by a Shimadzu UV-2450 spectrophotometer, using 10 mm quartz cells. PBS 9.5×10^{-4} and 1.8×10^{-3} M stock solutions of the HPTSC*-Fe and HPTSC*-Co complexes, respectively, were prepared and measured at 0, 48, 72 and 168 h. X-band EPR spectra were measured by using a Bruker EMX spectrometer, equipped with a Bruker ER 036TM NMR-teslameter and an Agilent 53150A microwave frequency counter. Variable temperature experiments were controlled by a Bruker ER 4131VT accessory by means of a liquid nitrogen evaporator, a heater and a BVT3000 temperature controller. Polycrystalline sample and frozen glassy solutions were used. In the last case, the stock PBS solution of HPTSC*-Fe and another one 1.3×10^{-3} M in DMSO were used. The standard quartz tubes were quickly frozen by hand in

a Dewar with liquid nitrogen before placing them in the spectrometer and then decreasing the temperature to 120 K. Simfonia program was used to perform the simulated spectra and graphics were carried out with Kaleidagraph [61, 62]. Experimental details are given in figure captions.

2.14. Statistical analysis.

All results are reported as means ± SD from n≥3. When comparing more than 2 groups, data were analyzed using analysis of variance (ANOVA). Post hoc analysis using the Student Neuman Keuls test was employed to detect differences between individual groups. In studies comparing only two experimental groups, data were analyzed with Student's t-test to determine significance of treatment effects. The level of statistical significance was taken as $p<0.05$.

3.-Results and discussion

3.1. Synthesis, characterization and stability of the compounds

The synthesis of thiosemicarbazonateiron(III), HPTSC-Fe and HPTSC*-Fe, and the analogous thiosemicarbazonatecobalt(III) derivatives, HPTSC-Co and HPTSC*-Co, has been carried out following the method summarized in Scheme 1. Note that, in the course of the reaction, the hydrazinic nitrogen atom deprotonates, except for extremely acid media pH < 2. Then, the TSC becomes into a thiosemicarbazonate ligand, and a new iminothiolato group is formed after a redistribution of the negative charge resting on the hydrazinic nitrogen. In the case of the HPTSC- containing compounds, HPTSC-Fe and HPTSC-Co, the preparation, characterization and stability have been previously reported [50, 63]. The procedure for the attainment of HPTSC*-Fe and HPTSC*-Co is described in the Experimental Section and some aspects are here discussed.

Compounds containing mononuclear $[M(TSC)_2]^+$ biscomplexes (M = Fe(III), Co(III); TSC = $PTSC^-$, $PTSC^{*-}$) are obtained. This fact is supported by the elemental analyses and FAB^+ measurements (Figures S1 and S2) shown in the present work. Besides, it is well established that their structures are constituted of distorted octahedral $[M(TSC)_2]^+$ biscomplexes, where tridentate NNS TSC ligands are placed in *mer* configuration. In this regard, an extensive crystallographic background on $[Fe(PTSC)_2]^+$ [63-66], $[Co(PTSC)_2]^+$ [51, 67-71], and $[Co(PTSC^*)_2]^+$ [72-74] claims for this proposal. Such a behavior contrasts with that reported for Cu(II) ions, where 1:1 $[Cu(TSC)]^+$ species are obtained, which use to exhibit dimeric, 1D or 2D nature in solid state. One can see, for instance, the crystal structures of HPTSC-Cu and HPTSC*-Cu, with 2D and dimeric arrangements, respectively, where nitrate and thiosemicarbazonate ligands act as bridges between the Cu(II) ions [32, 49].

The infrared measurements performed on the coordination compounds reveal strong analogies between the spectra of the metal complexes and changes of both graphics with respect to the spectrum of the free HPTSC* ligand (see Figure S3). These divergences comprise the presence of bands in the metal compounds around 1350 (broad and very strong) and 826 cm^{-1} (medium) attributed to ν_3 and ν_2 nitrate modes [75], which evidence the presence of counter ions in solid. Shifts of the bands at 996 and 927 cm^{-1} in the free ligand, assigned to vibration modes rich in ν(C=S) contribution, suggest the involvement of the thioamide sulfur in the linkage to metal ions. The band at 1520 cm^{-1} in the free ligand, attributed to a δ(NH) vibration mode, disappears in the complexes, in good agreement with the deprotonation of the TSC ligand on complexation. Furthermore, a new band arises in the 1605−1550 cm^{-1} region of the spectra of HPTSC*-Fe and HPTSC*-Co, which could be assigned to a ν(C=N) mode and

interpreted in terms of the formation of a new the azomethine nitrogen moiety upon chelation.

The HPTSC*-Fe powdered compound exhibits an inverted-axial type EPR spectrum at RT with g = 2.011 and $g_{\perp}$ = 2.156 (Figure S4, Experimental Section) characteristic of low-spin Fe(III) ions. It must be noticed that both the g-values are greater than that of the free electron one (g = 2.0023). These g-values are very similar to those of HPTSC-Fe (g_1 = 2.173, g_2 = 2.148, and g_3 = 2.018) and analogous thiosemicarbazonateiron(III) complexes [63]. The explanations for the relatively high g-value have been discussed elsewhere and could be related with the joined effects of the dipolar broadening, the low symmetry of the coordination polyhedron, the electronic delocalization in the highly conjugated TSC system and the influence of the lattice [63]. In fact, this behavior disappears in frozen solutions, where at least one of the g-values is lower than 2.0023, as expected for a pure d_{xy} ground-state (e.g., for a PBS solution, g_1 = 2.182, g_2 = 2.136, g_3 = 2.001, Figure S5). The PTSC-Fe compound, whose spectrum in DMSO is provided in Figure S6 for comparative purposes, exhibits a similar trend [63]. The g-values for the EPR spectra in frozen solutions are close to those reported for analogous TSC-Fe(III) compounds, as the Fe(III) derivatives of Triapine ® [76-80].

The evolution of the UV-vis spectrum with time for the HPTSC*-Co complex (Figure S7) reveals no relevant changes for 168 h. The stability of thiosemicarbazonecobalt(III) compounds in biological or analogous media has been discussed [46, 50, 81]. In the case of HPTSC*-Fe, only slight variations are observed (Figures S8 and S9). These small changes mainly affect the band at 597 nm in the fresh solution, which shifts to higher energies and exhibits a small increase in intensity with time. The origin of these changes is not clear. In this regard, the chemistry of pyridine-2-carbaldehyde thiosemicarbazoneiron analogues in aqueous solutions has been extensively

investigated, and different phenomena as self-reduction processes from Fe(III) to Fe(II) species [64, 82], further re-oxidation of the Fe(II) ones to form Fe(III) complexes with reduction of dioxygen [83-87] and even the acid-base behavior with changes in the band around 600 nm [88-90] have been reported. Anyway, the presence of a unique species is detected by EPR for 168 h (Figure S10), corresponding to the low spin Fe(III) species described above. These results as a whole suggest that compounds are essentially stable in the PBS media used in the biological studies.

3.2. Impact of thiosemicarbazones treatment on colon cancer (HT-29 and SW480)

TSCs are compounds with high attractive interest due to their anticancer effects, which are clearly affected by their structures and interaction with metals [60, 91]. Toxic levels of oxidative stress in tumor cells induce their cell death. For this reason, the use of TSCs to elevate ROS production in tumor cells may be potentially effective in cancer therapies [31-33]. In this regard, TSCs combined with transition metal ions are associated with activate cancer cell apoptosis and have been developed to decrease the severity of cancer in patients [92]. Mechanistically, TSCs are associated with the formation of redox-active metal complexes and the production of reactive oxygen species by the Fenton reaction. This mechanism is especially significant due to the emerging new targets in anticancer oxidative therapy. For this reasons, in this study the effect of two types of TSCs, HTPSC and HTPSC*, combined with Cu(II), Fe(III) and Co(III) metal ions on the viability of colon cancer cell lines is evaluated, together with the implication of oxidative stress.

Human colon cells are particularly suitable for cytotoxicity study because of their higher sensitivity to an increased ROS levels due to their higher basal level [93]. It is known that cancer cells operate under basal levels of ROS higher than those in normal cells

and, therefore, they become vulnerable to chemotherapeutic agents or redox active agents, such as metal complexes [94]. SW-480 is a line with a *KRAS* mutated and HT-29 *KRAS* is wild and, due to this, the susceptibility to the action of HPTSC is different, such as was evaluated by our research group in previous studies [49].

In order to evaluate the antiproliferative activity, colon cancer cells HT-29 and SW480 were incubated during 24 h with free TSCs (HPTSC and HPTSC*) and their coordination compounds with Cu(II), Fe(III) and Co(III) ions. The colon cancer cells were also incubated with the antitumor drug oxaliplatin, an effective agent for the treatment of colorectal cancer [95-97]. Furthermore, the effect of the TSCs compounds and oxaliplatin on the non-tumor CCD-112 cell line was evaluated. The results of the cytotoxicity assayed by MTT, in terms of IC50 values, are shown in Table 1. All the compounds showed antiproliferative effect after 24 h of treatment. The IC50 values of these compounds were lower than the results obtained with oxaliplatin. In all cases, the IC50 of the studied compounds in non-tumor (CCD-112) cells were significantly higher than the observed in tumor cells. These results indicate a high antiproliferative activity of the HPTSC and HPTSC* ligands and their metal complexes, selective against tumor cells and greater than that exhibited by oxaliplatin in the same experimental conditions.

A difference in the cytotoxicity was observed depending on the coordinated metal ion. The HPTSC and HPTSC* free ligands exhibited cytotoxicity with IC50 > 20 μM, similar to that obtained by other authors in the HT-29 cell line [98] and with a cell line-dependent effect higher in SW-480. The coordination of Cu(II) ions to HPTSC and HPTSC* increased the antiproliferative activity against both colon cancer cell lines with IC50 < 6 μM. In fact, all the HPTSC*-metal derivatives exhibit lower IC50 values than the free ligand. However, this fact is not valid for the HPTSC ones. Methylation increases the antiproliferative activity of the metal complexes, in an opposite way to that

in the free ligands. On the other hand, the cytotoxic effects for the Fe(III) and Co(III) compounds were significantly lower than those exhibited by the Cu(II) derivatives and lower than the results reported by other authors, as the IC50 values indicate [77, 92, 99-102]. The results of the HPTSC system against SW-480 cells roughly exhibit the same trends observed for inhibitory dose studies on melanoma B16F10 cells [64]. The mentioned studies reported a general cytotoxicity for the free ligands greater than that here obtained. The structure of the TSCs ligands is determinant in the cytotoxic effect. Thus, the metal complexes containing HPTSC* shows more cytotoxicity than the analogous compounds with HPTSC.

The selective activity against tumor cells was evaluated by comparing the cytotoxicity effect of TSC against human normal colon cell line (CCD 112). The results are showed in Table 1. The HPTSC and HPTSC* ligands, and their metal complexes, showed a greater toxicity in the cancer cell types than in normal cells. The higher selectivity against the cancer cells (HT-29, SW-480) was showed by the HPTSC-Cu and HTPSC*-Cu. The IC50 of HPTSC-Cu was 11.8 fold in normal cells than cancer cells and of the 13 fold for HPTSC*-Cu. The lower selectivity was observed for the free TSCs ligands (HTPSC and HPTSC*) and HPTSC-Fe. These results suggest the possible use as anti-cancer agents of HPTSC-Cu for their selective and cytotoxic effects.

3.3. Effect of metal-thiosemicarbazone treatment on antioxidant and redox state of colon cancer cells

Cancer cells operate under substantially higher level of intrinsic oxidative stress than normal cells, resulted of the oncogenic transformation. Because of the high ROS levels, cancer cells are more susceptible to show an increase in oxidative stress through TSC-metal complexes action. Deregulation of the endogenous antioxidant systems including

antioxidant enzymes as SOD or cellular redox systems, GSH/GSSG and Trx–TrxR, causes many alterations that lead to the induction of oxidative stress and apoptosis in cancer cells [100].

The SOD enzymes dismute the superoxide radical being the first defense against oxidative stress in the cell. The increment in their activity is a response to an increase in oxidative stress and could be associated with cytotoxicity in cancer cells. The mechanism of the activity of TSC-metal complexes depends on their redox properties, leading to formation of ROS [103]. Our results indicate that HPTSC*- Cu cytotoxicity could be mediated by the superoxide radical, such as showed significant increase ($p < 0.001$) in the SOD activity, being higher the cytotoxic effect in SW480 cell (Figure 1). However, the mechanisms of TSC derivatives containing Fe(III) ions could involve other species generated by Fenton reaction, such as hydroxyl radical, hence no increase in SOD activity is observed. On the other hand, the cytotoxicity of the Co(III) compounds is lesser, except for HPTSC-Co, than that exhibited by the other metal-complexes, which could be due to processes with no relation with ROS species.

The principal systems for maintenance of the intracellular redox status are the TRX–TRXr system and the GSH/GSSG ratio. The TRX protein could be decreased by the enzyme TRX reductases (TRXr) [104, 105] and the inhibition of TRX could have pro-apoptotic effects in cancer cells [106, 107]. The treatment of HT-29 and SW-480 with HPTSC produces changes in the concentration of TRX, but no changes are observed with HPTSC* (Figure 2). A decrease in the levels of TRX protein was observed because of the treatment with the different TSCs-metal compounds, highlighting the decrease observed in HT-29 cell in presence of the HPTSC-Cu(II).

The GSH/GSSG redox couple has been the traditional marker for the characterization of oxidative stress, because of its direct roles as antioxidants and cellular protectors. The

HT-29 cell line significantly decreases GSH/GSSG levels ($p < 0.05$) when treated with the studied TSC ligands and their metal complexes (Figure 3). In the case of the SW-480 cell line, the levels of GSH decrease significantly ($p<0.05$), except for the cells incubated with the HPTSC-Co complex. The maximum decrease occurs when the cells are treated with Cu(II) complexes, in good agreement with previously reported studies on the interaction of HPTSC-Cu and HPTSC*-Cu with GSH [30, 49, 108]. These results show that the HPTSC linked to the studied metal ions elevates the oxidative stress resulting in an oxidation of the reduced form of GSH to give glutathione disulfide (GSSG). All of these processes lead to an overall depletion of GSH and could give rise to mitochondrial dysfunction and cell death [10, 33, 109].

The reactivity of TSC-metal complexes against GSH is, at least in part, related with the redox potential of the compounds. The redox potentials $E^{o}_{Cu(II)TSC/Cu(I)TSC}$ and $E^{o}_{Fe(III)TSC/Fe(II)TSC}$ for complexes derived from pyridine-2-carbaldehyde thiosemicarbazone or quite similar ligands have been described in the Literature. The usual published E^{o} ranges are (+2) – (−230) mV for E^{o}_{Cu} and (+242) – (−3) mV for E^{o}_{Fe} [35, 83, 86, 99, 100,110-113]. All of them are more positive than $E^{o}_{GSH/GSSG}$ = –240 mV [114] and, therefore, redox reactions occur. The $E^{o}_{Co(III)TSC/Co(II)TSC}$ acquires more negative values, E^{o}_{Co} < –500 mV [115-117] and the experimental evidence is that no reaction of Co(III) species with GSH takes place [114], in good agreement with the stability and inertness of low-spin $3d^6$ Co(III) complexes. The methylation on the terminal thioamide nitrogen atom has variable influence in the value of E^{o}, depending on the TSC ligand [112, 115].

3.4. Effect of thiosemicarbazone-metal complexes on biomarkers of oxidative stress and apoptosis markers in cancer colon cells

The increase in ROS levels results in a major damage to biomolecules and this is involved in the evolution of tumor cells [118]. In this regard, we have evaluated the cell damage quantifying the biomarkers of protein, lipid and DNA damage as indicators of ROS levels. In this sense, the results show that HTPSC coordinated to metals increases the oxidative stress, such as observed in the greater amounts of biomarkers of protein (carbonyl groups), lipid (MDA) and DNA damage (8-OHdG/dG). An increase is observed in the levels of carbonyl groups (CGs) when both lines were incubated with the HPTSC and HPTSC* ligands coordinated to metals. Besides, the protein oxidative damage is dependent of the cell line treated. CGs levels are significantly higher in the *KRAS* mutated-SW-480 cells than in the wild type HT-29 where the treatments used were HPTSC-Cu ($p<0.001$), HPTSC-Fe ($p<0.05$), and HPTSC*-Cu ($p<0.001$), HPTSC*-Fe ($p<0.05$) HPTSC*-Co ($p< 0.001$) (Figure 4). The lipid peroxidation was evaluated by measuring the levels of MDA. HPTSC and HPTSC* free ligands and their metal complexes are leading to high levels of MDA in the cell line SW-480. Highlight the treatment with HPTSC, HPTSC-Co, HPTSC*, HPTSC*-Cu and HPTSC-Co compounds that significantly increased the MDA levels ($p<0.05$) (Figure 5). These results indicate an increase in the level of oxidative stress in cancer cells, possibly due to the removal of metals by HPTSC and HPTSC*. It would lead to the formation of redox-active complexes that produce an increased in the levels of ROS increasing the damage to lipids and protein. Therefore, the amplification of ROS levels by the evaluated TSCs compounds could be the mechanism by which could induce tumor regression, similar to other chemotherapeutic compounds [30-33].

Moreover, the HPTSC treatment increased the DNA oxidative damage, evaluated as levels of 8OHdG/2dG in both cell lines, but HPTSC* increased only in HT-29 cell line (Table 2). The oxidation of the DNA bases is increased significantly when the cells are

treated with the ligands coordinated to Cu(II) ($p<0.001$) in both cell lines. The effect of the treatment with the other metal ions was significantly lower. Marked differences between cell lines are found when they are treated with the HPTSC ligand coordinated to Cu(II) ($p<0.001$), Co(III) ($p<0.05$) and Fe(III) ($p<0.05$) (Table 2). This increase in the levels of 8OHdG could be involved in their cytotoxic effect. The ability of these compounds to induce DNA damage, which not is repaired could interfere with DNA replication and induce an increase in mitochondrial ROS. As a whole, these factors could contribute to apoptosis and autophagy in cancer cells [119-120].

One of the ways of achieving apoptosis is the activation of caspases, proteins mediated by oxidative stress. Caspases are protease enzymes involved in the initiation and execution of apoptosis process and their levels are used as prognostic factor in CRC [120]. In this study, the effects of the TSC-metal complexes on the levels of the initiator caspase 9 and the effector caspase 3 in the cancer lines were evaluated (Table 2). Apoptosis resulted from the treatment with TSC-metal compounds was detected in both cell lines. The levels of caspase 9 were higher than those of caspase 3 in both cell lines and the effect of treatment with TSCs was dependent on the metal coordinated. The treatment of HPTSC and HPTSC* linked to Cu(II) ions significantly increased ($p<0.05$) the levels of caspase 3 and caspase 9 in both cell lines, being the highest ones for HPTSC-Cu(II) in the SW-480 cell line (Table 2). The effect of the TSCs coordinated to Fe(III) and Co(III) ions was lower than that observed with Cu(II), but significant with respect to non-treated cells, a similar behavior to that observed with the DNA damage. In the same way, SW-480 cells treated with TSCs coordinated to Cu(II) ions exhibit a histones index higher ($p<0.05$) than that in HT-29 (Table 2). These results indicate that the complexes with HPTSC and HPTSC* showed excellent cytotoxicity profiles against

the two human colon cancer cell lines. Interestingly, the major effect was observed in SW480 line cell that have *KRAS* mutated present in approximately 40% of all CRC.

In summary, the results suggest that the complex HPTSC*- Cu leads to a significant anticancer selectivity, overcomes in mutated *KRAS* cells by the mechanism of ROS mediated apoptosis and, therefore, it could be considered in an effective strategy for colon cancer treatment with poor response to *EGFR*- inhibiting drugs characteristic of mutated *KRAS* cells.

3.5. Reactivity with cytochrome c and myoglobin.

The binding to human proteins can alter the uptake and efficiency of drugs. In this sense, the interaction between TSCs, and their metal complexes, with albumin has been previously studied [121, 122]. The reaction with hemoglobin and myoglobin has been also explored and the influence in the biological activity, with formation of methemoglobin and metmyoglobin and induction of hypoxia, discussed elsewhere [83, 122-125]. On the other hand, it has been reported the presence of an heme EPR signal in peripheral blood mononuclear cells obtained from patients treated with Triapine ® [76], attributed to cytochrome c released from damaged mitochondria by the action of ROS generated by copper- and iron-Triapine complexes.

For these reasons, ESI experiments have been carried out to study the interaction of the metal complexes on cytochrome c and myoglobin. The results are given in Supporting Information (Figures S11-S14) and suggest that only the Fe(III) derivatives exhibit appreciable interactions with cytochrome c and myoglobin. Anyway, these interactions seem to be low. No interactions are observed for the Co(III) complexes. Regarding this, Cu(II) complexes with the same ligands showed low interaction, while the free TSCs did not link to the same proteins, as previously reported [49]. In that case, the cysteine-

rich cytochrome c seemed to provoke a release of the Cu(II) ions from their bindings to the TSCs, in good agreement with the existence of previous reduction processes. As a result, the Cu(I) ions moved from the TSC to the cytochrome c and were retained by it. This behavior was not observed for the reaction with myoglobin, a protein without cysteine amino acids. No metal release is observed in the Fe(III) and Co(III) compounds here reported, which can be related with the marked difference in coordinative behavior and metal chemistries. As it has been described in Section 3.1, Fe(III) and Co(III) ions give rise to coordinative saturated distorted octahedral $[M(TSC)_2]^+$ biscomplexes, whose reduction with cell thiols, at least in the case of $[Fe(TSC)_2]^+$, generates relatively hard Fe(II) ions that are strongly bonded to the tridentate TSC ligand through the $N_{pyridine}$, $N_{azomethine}$ and $S_{thioamide}$ atoms. On the contrary, Cu(II) mainly stabilizes $[Cu(TSC)]^+$ entities due to the Jahn-Teller effect [104,126], where Cu(II) ions are also bonded to tridentate NNS TSC ligand. However, the reaction with reductants, as cell thiols, originates soft Cu(I) ions only linked to the TSC through the thioamide sulfur atom, as crystallographic studies show [12, 127, 128]. Then, the stability of the TSC-Cu(I) species drastically decreases with respect to the TSC-Cu(II) ones, and the Cu(I) metal ion is released when other soft ligands, as cysteine-containing molecules, are present.

Despite one could consider the positively charged and coordinately saturated $[M(TSC)_2]^+$ entities to be linked to the proteins through electrostatic interactions, no clear explanation is found for the affinity of cytochrome c and myoglobin to $[Fe(TSC)_2]^+$ and not for the analogous $[Co(TSC)_2]^+$. Indeed, it could suggest the influence of the inertness of Co(III) ions and, therein, a chemically complex behavior.

Conflicts of interest

None.

Table of Abbreviations:

ATCC	American tissue cell collection	HPTSC*-Fe	$Fe(PTSC^*)_2(NO_3)(H_2O)_3$
ATR	Attenuated total reflectance	HPTSC*-Co	$Co(PTSC^*)_2(NO_3)(H_2O)_3$
CGs	carbonyl groups	HPTSC*-Cu	$Cu(PTSC^*)(NO_3)$
CRC	colorectal cancer	MDA	malondialdehyde
DMEM	Dulbecco´s modified Eagle´s medium	MEM	Modified Eagle´s medium
DMSO	dimethyl sulfoxide	MTT	3-(4,5-dimethylthiazol-2-yl)-2,5-diphenyltetrazolium bromide
EPR	Electron paramagnetic resonance	NBA	*m*-nitrobenzyl alcohol
FAB	Fast atom bombardment	PBS	phosphate buffer saline
FBS	fetal bovine serum	PTSC	Deprotonated HPTSC
GSH	reduced glutathione	PTSC*	Deprotonated HPTSC*
GSSG	oxidized glutathione	ROS	reactive oxygen species
HPLC	High performance liquid chromatography	RT	room temperature
HPTSC	pyridine-2-carbaldehyde thiosemicarbazone	SOD	superoxide dismutase
HPTSC*	pyridine-2-carbaldehyde 4N-methylthiosemicarbazone	TNB	2-nitro-5-thiobenzoate
HPTSC-Fe	$Fe(PTSC)_2(NO_3)(H_2O)_3$	TRX	thioredoxin
HPTSC-Co	$Co(PTSC)_2(NO_3)$	TRXr	thioredoxin reductase
HPTSC-Cu	$Cu(PTSC)(NO_3)$	TSC	thiosemicarbazone

References

1. M. Araghi, I. Soerjomataram, M. Jenkins, J. Brierley, E. Morris, F. Bray, M. Arnold, Int. J. Cancer. 144 (2019) 2992–3000.

2. M. Herreros-Villanueva, M. Rodrigo, M. Claver, Muñiz, P. Lastra E, C. García-Girón, M.J. Coma Corral, Mol. Biol. Rep. 38 (2011) 1315–1320.

3. M. Herreros-Villanueva, N. Gomez-Manero, P. Muñiz, C. García-Girón, M.J. Coma del Corral, Mol. Biol. Rep. 38 (2011) 1347–1351.

4. M. Morkel, P. Riemer, H. Bläker, C. Sers, Oncotarget. 6 (2015) 20785–20800.

5. C. Therkildsen, T.K. Bergmann, T. Henrichsen-Schnack, S. Ladelund, M. Nilbert, Acta Oncol. 53 (2014) 852–864.

6. M. Russo, G. Siravegna, L.S. Blaszkowsky, G. Corti, G. Crisafulli, L.G. Ahronian, B. Mussolin, E.L. Kwak, M. Buscarino, L. Lazzari, E. Valtorta, M. Truini, N.A. Jessop, H.E. Robinson, T.S. Hong, M. Mino-Kenudson, F. Di Nicolantonio, A. Thabet, A. Sartore-Bianchi, S. Siena, A.J. Iafrate, A. Bardelli, R.B. Corcoran, Cancer Discov. 6 (2016) 147–153.

7. A. Yilmazer, Biotechnol. Rep. (Amst). 17 (2017) 24–30.

8. M. Cavia-Saiz, P. Muñiz, R. De Santiago, M. Herreros-Villanueva, C. Garcia-Giron, A.S. Lopez, M.J. Coma-Corral, Biochem. Cell Biol. 90 (2012) 173–178.

9. N. Margetis, M. Kouloukoussa, K. Pavlou, S. Vrakas, T. Mariolis-Sapsakos, In Vivo. 31 (2017) 527–542.

10. F. Bisceglie, S. Pinelli, R. Alinovi, P. Tarasconi, A. Buschini, F. Mussi, A. Mutti, G. Pelosi, J Inorg Biochem. 116 (2012) 195–203.

11. T.S. Lobana, R. Sharma, G. Bawa, S. Khanna, Coord. Chem. Rev. 253 (2009) 977–1055.

12. J. García-Tojal, R. Gil-García, P. Gómez–Saiz, M. Ugalde, Curr. Inorg. Chem. 1 (2011) 189–210.

13. Y. Yu, D.S. Kalinowski, Z. Kovacevic, A.R. Siafakas, P.J. Jansson, C. Stefani, D.B. Lovejoy, P.C. Sharpe, P. V. Bernhardt, D.R. Richardson, J. Med. Chem. 52 (2009) 5271–5294.

14. D.J. Lane, T.M. Mills, N.H. Shafie, A.M. Merlot, R. Saleh Moussa, D.S. Kalinowski, Z. Kovacevic, D.R. Richardson, BBA - Rev. Cancer. 1845 (2014) 166–181.

15. B.A. Fang, Ž. Kovačević, K.C. Park, D.S. Kalinowski, P.J. Jansson, D.J.R. Lane, S. Sahni, D.R. Richardson, Biochim. Biophys. Acta - Rev. Cancer. 1845 (2014) 1–19.

16. N. Seebacher, D.J.R. Lane, D.R. Richardson, P.J. Jansson, Free Radic. Biol. Med. 96 (2016) 432–445.

17. D.S. Kalinowski, C. Stefani, S. Toyokuni, T. Ganz, G.J. Anderson, N. V Subramaniam, D. Trinder, J.K. Olynyk, A. Chua, P.J. Jansson, S. Sahni, D.J.R. Lane, A.M. Merlot, Z. Kovacevic, M.L.H. Huang, C.S. Lee, D.R. Richardson, Biochim. Biophys. Acta - Mol. Cell Res. 1863 (2016) 727–748.

18. J.F. de Oliveira, T.S. Lima, D.B. Vendramini-Costa, S.C.B. de Lacerda Pedrosa, E.A. Lafayette, R.M.F. da Silva, S.M.V. de Almeida, R.O. de Moura, A.L.T.G. Ruiz, J.E. de Carvalho, M.D.C.A. de Lima, Eur J Med Chem. 136 (2017) 305–314.

19. F.A. French, E.J. Jr Blanz, Cancer Res. 25 (1965) 1454–1458.

20. R.W. Brockman, R.W. Sidwell, G. Arnett, S. Shaddix, Proc. Soc. Exp. Biol. Med. 133 (1970) 609–614.

21. M.F. Zaltariov, M. Hammerstad, H.J. Arabshahi, K. Jovanović, K.W. Richter, M. Cazacu, S. Shova, M. Balan, N.H. Andersen, S. Radulović, J. Reynisson, K.K. Andersson, V.B. Arion, Inorg. Chem. 56 (2017) 3532–3549.

22. I.H. Hall, C.B. Lackey, T.D. Kistler, R.W. Jr Durham, E.M. Jouad, M. Khan, X.D. Thanh, S. Djebbar-Sid, O. Benali-Baitich, G.M. Bouet, Pharmazie. 55 (2000) 937–941.

23. F. Bisceglie, M. Baldini, M. Belicchi-Ferrari, E. Buluggiu, M. Careri, G. Pelosi, S. Pinelli, P. Tarasconi, Eur. J. Med. Chem. 42 (2007) 627–634.

24. J.A. Ludwig, G. Szakács, S.E. Martin, B.F. Chu, C. Cardarelli, Z.E. Sauna, N.J. Caplen, H.M. Fales, S.V. Ambudkar, J.N. Weinstein, M.M. Gottesman, Cancer Res. 66 (2006) 4808–4815.

25. C.P. Wu, S. Shukla, A.M. Calcagno, M.D. Hall, M.M. Gottesman, S.V. Ambudkar, Mol. Cancer Ther. 6 (2007) 3287–3296.

26. B.M. Zeglis, V. Divilov, J.S. Lewis. J. Med. Chem. 54 (2011) 2391–2398.

27. B. García, J. Garcia-Tojal, R. Ruiz, R. Gil-García, S. Ibeas, B. Donnadieu, J.M. Leal, J. Inorg. Biochem. 102 (2008) 1892–1900.

28. R. Ruiz, B. García, J. Garcia-Tojal, N. Busto, S. Ibeas, J.M. Leal, C. Martins, J. Gaspar, J. Borras, R. Gil-Garcia, M. Gonzalez-Alvarez, J. Biol. Inorg. Chem. 15 (2010) 515–532.

29. R. Gil-Garcia, M. Ugalde, N. Busto, H.J. Lozano, J.M. Leal, B. Perez, G. Madariaga, M. Insausti, L. Lezama, R. Sanz, L.M. Gómez-Sainz, B. Garcia, J. Garcia-Tojal, Dalton Trans. 45 (2016) 18704–18718.

30. L.A. Saryan, K. Mailer, C. Krishnamurti, W.E. Antholine, D.H. Petering, Biochem. Pharmacol. 30 (1981) 1595–1604.

31. J. García-Tojal, A. García-Orad, J.L. Serra, J.L. Pizarro, L. Lezama, M.I. Arriortua, T. Rojo, J. Inorg.Biochem. 75 (1999) 45–54.

32. P. Gómez-Saiz, J. García-Tojal, M.A. Maestro, F.J. Arnaiz, T. Rojo, Inorg. Chem. 41 (2002) 1345–1347.

33. K. Malarz, A. Mrozek-Wilczkiewicz, M. Serda, M. Rejmund, J. Polanski, R. Musiol, Oncotarget. 9 (2018) 17689–17710.

34. S. Kallus, L. Uhlik, S. van Schoonhoven, K. Pelivan, W. Berger, E.A. Enyedy, T. Hofmann, P. Heffeter, C.R. Kowol, B.K. Keppler, J. Inorg. Biochem. 190 (2019) 85–97.

35. C.R. Kowol, R. Trondl, P. Heffeter, V.B. Arion, M.A. Jakupec, A. Roller, M. Galanski, W. Berger, B.K. Keppler, J. Med. Chem. 52 (2009) 5032–5043.

36. K.C. Agrawal, A.C. Sartorelli, in: G.P. Ellis, G.B. West (Ed.), Progress in Medicinal Chemistry, vol. 15, The chemistry and biological activity of α-(N)-heterocyclic carboxaldehyde thiosemicarbazones, Elsevier/North-Holland Biomedical Press, Amsterdam, 1978, pp. 321–356.

37. A.I. Matesanz, P. Souza, Mini Rev. Med. Chem. 9 (2009) 1389–1396.

38. M.N.M. Milunovic, É.A. Enyedy, N.V. Nagy, T. Kiss, R. Trondl, M.A. Jakupec, B.K. Keppler, R. Krachler, G. Novitchi, V.B. Arion, Inorg. Chem. 51 (2012) 9309–9321.

39. A. Dobrova, S. Platzer, F. Bacher, M.N.M. Milunovic, A. Dobrov, G. Spengler, É.A. Enyedy, G. Novitchi, V.B. Arion, Dalt. Trans. 45 (2016) 13427–13439.

40. Y. Gou, J. Wang, S. Chen, Z. Zhang, Y. Zhang, W. Zhang, F. Yang, Eur. J. Med. Chem. 123 (2016) 354–364.

41. F.N. Akladios, S.D. Andrew, C.J. Parkinson, Biometals. 29 (2016) 157–70.

42. Y. Fu, Y. Liu, J. Wang, C. Li, S. Zhou, Y. Yang, P. Zhou, C. Lu, C. Li, Oncol. Rep. 37 (2017) 1662–1670.

43. H. Karlsson, M. Fryknäs, S. Strese, J. Gullbo, Oncotarget. 8 (2017) 30217–30234.

44. M.N.M. Milunović, A. Dobrova, G. Novitchi, N. Gligorijević, Eur. J. Inorg. Chem. (2017) 4773–4783.

45. A. Sirbu, O. Palamarciuc, M.V. Babak, J.M. Lim, K. Ohui, E.A. Enyedy, S. Shova, D. Darvasiová, P. Rapta, W.H. Ang, V.B. Arion, Dalton Trans. 46 (2017) 3833–3847.

46. T.R. Todorović, J. Vukasinovic, G. Portalone, S. Suleiman, N. Gligorijević, S. Bjelogrlic, K. Jovanovic, S. Radulović, K. Anđelković, A. Cassar, N.R. Filipović, P. Schembri-Wismayer, Med. Chem. Commun. 8 (2017) 103–111.

47. C.R. Kowol, W. Miklos, S. Pfaff, S. Hager, S. Kallus, K. Pelivan, M. Kubanik, É.A. Enyedy, W. Berger, P. Heffeter, B.K. Keppler, J. Med. Chem. 59 (2016) 6739–6752.

48. K. Ishiguro, Z.P. Lin, P.G. Penketh, K. Shyam, R. Zhu, R.P. Baumann, Y. Zhu, A.C. Sartorelli, T.J. Rutherford, E.S. Ratner, Biochem. Pharmacol. 91 (2014) 312–322.

49. J. García-Tojal, R. Gil-García, V.I. Fouz, G. Madariaga, L. Lezama, M.S. Galletero, J. Borrás, F.I. Nollmann, C. García-Girón, R. Alcaraz, M. Cavia-Saiz, P. Muñiz, Ò. Palacios, K.G. Samper, T. Rojo, J. Inorg. Biochem. 180 (2018) 69–79.

50. R. Gil–García, R. Fraile, B. Donnadieu, G. Madariaga, V. Januskaitis, J. Rovira, L. González, J. Borrás, F.J. Arnáiz, J. García–Tojal, New J. Chem. 37 (2013) 3568–3580.

51. J. García-Tojal, García-Orad, A Díaz, J.L. Serra, M.K. Urtiaga, M.I. Arriortua, T. Rojo, J. Inorg. Biochem. 84 (2001) 271–278.

52. F.E. Anderson, C.J. Duca, J.V. Scudi, J. Am. Chem. Soc. 73 (1951) 4967–4968.

53. A.G. Bingham, H. Bögge, A. Müler, E.W. Ainscough, A.M. Brodie, J. Chem. Soc., Dalton Trans. (1987) 493–499.

54. D.X. West, G.A. Bain, J.S. Saleda, A.E. Liberta, Transition Met. Chem. 16 (1991) 565–572.

55. D.X. West, G.A. Bain, R.I. Butcher, J.P. Jasinskin, R.Y. Pozniakiv, J. Valdés–Martínez, R.A. Toscano, S. Hernández–Ortega, Polyhedron 15 (1996) 665–674.

56. R. Noto, P. Lo Meo, M. Gruttadauria, G. Werber, J. Heterocyclic. Chem. 33 (1996) 863–872.

57. J.M. McCord, I. Fridovich, J. Biol. Chem. 243 (1968) 5753–5760.

58. A. Holmgren, M. Björnstedt. Methods Enzymol. 252 (1995) 199–208.

59. R.L. Levine, E.R. Stadtman, Exp. Gerontol. 36 (2001) 1495–1502.

60. D. Grotto, L.D. Santa Maria, S. Boeira, J. Valentini, M.F. Charão, M. Moro, P.C. Nascimento, V.J. Pomblum, S.C. Garcia, J. Pharm. Biomed. Anal. 43 (2007) 619–624.

61. WINEPR SimFonia v1.25, Bruker Analytische Messtecnik GmßH, (1996).

62. KaleidaGraph v4.1; Synergy Software: Reading, Pensilvania (EE.UU.), (1986–2009).

63. J. Garcia-Tojal, J.L. Pizarro, L. Lezama, M.I. Arriortua, T. Rojo, Inorg. Chim. Acta. 278 (1998) 150–158.

64. J. García-Tojal, B. Donnadieu, J.P. Costes, J.L. Serra, L. Lezama, T. Rojo, Inorganica Chim. Acta. 333 (2002) 132–137.

65. T. Sarkar, S. Banerjee, A. Hussain, RSC Adv. 5 (2015) 29276–29284.

66. C.R. Kowol, R. Berger, R. Eichinger, A. Roller, M.A. Jakupec, P.P. Schmidt, V.B. Arion, B.K. Keppler, J. Med. Chem. 50 (2007) 1254–1265.

67. K.N. Akatova, T.N. Tarkhova, N.V. Belov, Kristallografiya (Russ.) (Crystallogr.Rep.) (1973) 263–268.

68. K.N. Akatova, T.N. Tarkhova, S.L. Ginzburg, M.G. Neigauz, L.A. Novakovskaya, Kristallografiya (Russ.) (Crystallogr.Rep.) 19 (1974) 383–385.

69. S.K. Chattopadhyay, T. Banerjee, P. Roychoudhury, T.C.W. Mak, S. Ghosh, Transition Met. Chem. 22 (1997) 216–219.

70. H.-S. Wang, L. Huang, Z.-F. Chen, X.-W. Wang, J. Zhou, S.-M. Shi, H. Liang, K.-B. Yu Acta Crystallogr., Sect. E: Struct. Rep. Online 60 (2004) m344.

71. G. Mahmoudi, A.V. Gurbanov, S. Rodríguez-Hermida, R. Carballo, M. Amini, A. Bacchi, M.P. Mitoraj, F. Sagan, M. Kukułka, D.A. Safin, Inorg Chem. (2017) 21;56(16):9698–9709.

72. J. Castineiras, D.X. West, H. Gebremedhin, T.J. Romack, Inorg. Chim. Acta 216 (1994) 229−236.

73. M.R. Bermejo, A.M. Gonzalez-Noya, M. Martinez-Calvo, R. Pedrido, M.J. Romero, M.I. Fernandez, M. Maneiro, Z. Anorg. Allg. Chem. 633 (2007) 807–813.

74. X.F. Zhu, Y.H. Fan, Q. Wang, C.L. Chen, M.X. Li, J.W. Zhao, J. Zhou, J. Russ, Coord. Chem. 38 (2012) 478–483.

75. K. Nakamoto, Infrared and raman spectra of inorganic and coordination compounds, 6th Ed., John Wiley & Sons, New Jersey, 2009.

76. J.M. Kolesar, W.R. Schelman, P.G. Geiger, K.D. Holen, A.M. Traynor, D.B. Alberti, J.P. Thomas, C.R. Chitambar, G. Wilding, W.E. Antholine, J. Inorg. Biochem. 102 (2008) 693–698.

77. E.A. Akam, T.M. Chang, A. V Astashkin, E. Tomat, Metallomics. 6 (2014) 1905–12.

78. K. Pelivan, W. Miklos, S. van Schoonhoven, G. Koellensperger, L. Gille, W. Berger, P. Heffeter, C.R. Kowol, B.K. Keppler, J. Inorg. Biochem. 160 (2016) 61–69.

79. D. Palanimuthu, R. Poon, S. Sahni, R. Anjum, D. Hibbs, H. Lin, P. V Bernhardt, D.S. Kalinowski, D.R. Richardson, Eur. J. Med. Chem. 139 (2017) 612–632.

80. W.E. Antholine, C.R. Myers, Int. J. Mol. Sci. 20 (2019) 3062, 1–8.

81. J.G. Deng, T. Li, G. Su, Q.P. Qin, Y. Liu, Y. Gou, J. Mol. Struct. 1167 (2018) 33–43.

82. A. Abras, H. Beraldo, E.O. Fantini, R.H.U. Borges, M.A. Da Rocha, L. Tosi, Inorg. Chim. Acta 172 (1990) 113 117.

83. W. Antholine, J. Knight, H. Whelan, D.H. Petering, Mol. Pharmacol. 13 (1977) 89–98.

84. J. Shao, B. Zhou, A.J. Di Bilio, L. Zhu, T. Wang, C. Qi, J. Shih, Y. Yen, Mol. Cancer Ther. 5 (2006) 586–592.

85. M.T. Basha, J. Bordini, D.R. Richardson, M. Martinez, P. V. Bernhardt, J. Inorg. Biochem. 162 (2016) 326–333.

86. P. V. Bernhardt, M.A. Gonzálvez, M. Martínez, Inorg. Chem. 56 (2017) 14284–14290.

87. S. Plamthottam, D. Sun, J. Van Valkenburgh, J. Valenzuela, B. Ruehle, J. Biol. Inorg. Chem. 24 (2019) 621–632.

88. H. Beraldo, L. Tosi, Inorg. Chim. Acta 75 (1983) 249–257.

89. R.H.U. Borges, E. Paniago, H. Beraldo, J. Inorg. Biochem. 65 (1997) 267–275.

90. É. A. Enyedy, N. V. Nagy, É. Zsigó, C.R. Kowol, V.B. Arion, B.K. Keppler, T. Kiss, Eur. J. Inorg. Chem. (2010) 1717–1728.

91. F.N. Akladios, S.D. Andrew, C.J. Parkinson, Bioorg. Med. Chem. 23 (2015) 3097–3104.

92. P. Heffeter, V.F.S. Pape, É.A. Enyedy, B.K. Keppler, G. Szakacs, C.R. Kowol, Antioxid. Redox Signal. 30 (2019) 1062–1082.

93. N. Yu, H. Zhu, Y. Yang, Y. Tao, F. Tan, Q. Pei, Y. Zhou, X. Song, Q. Tan, H. Pei, Oncotarget 8 (2017) 51478–51491.

94. G. Haklar, E. Sayin-Ozveri, M. Yüksel, A.O. Aktan, A.S. Yalçin, Cancer Lett. 165 (2001) 219–224.

95. S.W. Lowe, A.W. Lin, Carcinogenesis 31 (2000) 485-495.

96. I. Gourdier, M. Del Rio, L. Crabbé, L. Candeil, V. Copois, M. Ychou, C. Auffray, P. Martineau, N. Mechti, Y. Pommier, B. Pau, FEBS Lett. 529 (2002) 232-6.

97. D. Arango, A.J. Wilson, Q. Shi, G.A. Corner, M.J. Arañes, C. Nicholas, M. Lesser, J.M. Mariadason, L.H. Augenlicht, Br J Cancer. 91 (2004) 1931-46.

98. M. Valko, D. Leibfritz, J. Moncol, M.T. Cronin, M. Mazur, J. Telser, Int. J. Biochem. Cell Biol. 39 (2007) 44–84.

99. E.W. Ainscough, A.M. Brodie, W. A. Denny, G.J. Finlay, J.D. Ranford, J. Inorg. Biochem. 70 (1998) 175–185.

100. C.R. Kowol, P. Heffeter, W. Miklos, L. Gille, R. Trondl, L. Cappellacci, W. Berger, B.K. Keppler, J. Biol. Inorg. Chem. 17 (2012) 409–423.

101. S. Sandhaus, R. Taylor, T. Edwards, A. Huddleston, Y. Wooten, R. Venkatraman, R.T. Weber, A. González-Sarrías, P.M. Martin, P. Cagle, Y.C. Tse-Dinh, S.J. Beebe, N. Seeram, A.A. Holder, Inorg. Chem. Commun. 64 (2016) 45–49.

102. Z. Chen, J. Sun, T. Li, Y. Liu, S. Gao, X. Zhi, Biochem. Biophys. Res. Commun. 506 (2018) 114–121.

103. M. Valko, K. Jomova, C.J. Rhodes, K. Kuča, K. Musílek, Arch. Toxicol. 90 (2016) 1–37.

104. P.J. Jansson, P.C. Sharpe, P.V. Bernhardt, D.R. Richardson, J. Med. Chem. 53 (2010) 5759–5769.

105. J.A. Lessa, M.A. Soares, R.G. dos Santos, I.C. Mendes, L.B. Salum, H.N. Daghestani, A.D. Andricopulo, B.W. Day, A. Vogt, H. Beraldo, Biometals 26 (2013) 151–165.

106. J.M. Myers, Q. Cheng, W.E. Antholine, B. Kalyanaraman, A. Filipovska, E.S. Arnér, C.R. Myers, Free Radic. Biol. Med. 60 (2013) 183–194.

107. J. Zhang, X. Li, X. Han, R. Liu, J. Fang, Trends Pharmacol. Sci. 38 (2017) 794–808.

108. A. Santoro, B. Vileno, O. Palacios, M.D. Peris-Diaz, G. Riegel, C. Gaiddon, A. Krezel, P. Faller, Metallomics 11 (2019) 994–1004.

109. N. Traverso, R. Ricciarelli, M. Nitti, B. Marengo, A.L. Furfaro, M.A. Pronzato, U.M. Marinari, C. Domenicotti, Oxid. Med. Cell Longev. 2013 (2013), Article ID 972913, 10 pages.

110. W.E. Antholine, J.M. Knight, D.H. Petering, Inorg. Chem. 16 (1977) 569–574.

111. J.M. Knight, H. Whelan, D.H. Petering, J. Inorg. Biochem. 11 (1979) 327–338.

112. É.A. Enyedy, M.F. Primik, C.R. Kowol, V.B. Arion, T. Kiss, B.K. Keppler, Dalton Trans. 40 (2011) 5895–5905.

113. D.B. Lovejoy, D.M. Sharp, N. Seebacher, P. Obeidy, T. Prichard, C. Stefani, M.T. Basha, P.C. Sharpe, P.J. Jansson, D.S. Kalinowski, P.V. Bernhardt, D.R. Richardson, J. Med. Chem. 55 (2012) 7230–7244.

114. F.Q. Schafer, G.R. Buettner, Free Radic. Biol. Med. 30 (2001) 1191–1212.

115. P.V. Bernhardt, P.C. Sharpe, M. Islam, D.B. Lovejoy, D.S. Kalinowski, D.R. Richardson, J. Med. Chem. 52 (2009) 407–415.

116. C.G. Oliveira, P.I. Da S. Maia, M. Miyata, F.R. Pavan, C.Q.F. Leite, E.T. De Almeida, V.M. Deflon, J. Brazilian Chem. Soc. 25 (2014) 1848–1856.

117. I.S. Djordjević, J. Vukašinović, T.R. Todorović, J. Serbian Chem. Soc. 82 (2017) 301–310.

118. H.M. Kuznietsova, M.S. Yena, I.P. Kotlyar, O.V. Ogloblya, V.K. Rybalchenko, Scientific World Journal (2016) Article ID 2145753.

119. H. Yang, R. Villani, H. Wang, M.J. Simpson, M.S. Roberts, M. Tang, X. Liang, Exp. Clin. Cancer Res. 37 (2018) 266.

120. M. Asadi, D. Shanehbandi, T. Asvadi Kermani, Sanaat, Z.V. Zafari, S. Hashemzadeh, Asian Pac. J. Cancer Prev. 19 (2018) 1277–1280.

121. A.M. Merlot, S. Sahni, D.J. Lane, A.M. Fordham, N. Pantarat, D.E. Hibbs, V. Richardson, M.R. Doddareddy, J.A. Ong, M.L. Huang, D.R. Richardson, D.S. Kalinowski, Oncotarget 6 (2015) 10374-98.

122. P. Reimerová, J. Stariat, H. Bavlovič Piskáčková, H. Jansová, J. Roh, D.S. Kalinowski, M. Macháček, T. Šimůnek, D.R. Richardson, P. Štěrbová-Kovaříková, Anal. Bioanal. Chem. 411 (2019) 2383-2394.

123. W. Antholine, F. Taketa, J. Inorg. Biochem. 16 (1982) 145-154.

124. W. Antholine, F. Taketa, J. Inorg. Biochem. 20 (1984) 69-78.

125. P. Quach, E. Gutierrez, M.T. Basha, D.S. Kalinowski, P.C. Sharpe, D.B. Lovejoy, P.V. Bernhardt, P.J. Jansson, D.R. Richardson, Mol. Pharmacol. 82 (2012) 105-114.

126. A.E. Stacy, D. Palanimuthu, P.V. Bernhardt, D.S. Kalinowski, P.J. Jansson, D.R. Richardson, J. Med. Chem. 25 (2016) 8601–8620.

127. T.S. Lobana, Rekha, R.J. Butcher, A. Castiñeiras, E. Bermejo, P.V. Bharatam, Inorg. Chem. 45 (2006) 1535–1542.

128. T.S. Lobana, R. Sharma, A. Castiñeiras, R. Jay, Z. Anorg. Allg. Chem. 636 (2010) 2698–2703.

Scheme Captions

Scheme 1. Representation of the synthesis method of the complexes. The numbered asterisks indicate the chelating centers of the thiosemicarbazone ligands, i.e. pyridine (1), azomethine (2) and sulfur thioamide (3) atoms. The hydrazinic nitrogen is surrounded by a circle.

Figure Captions

Figure 1. SOD activity (U/mg prot) of HT-29 and SW-480 treated with the HPTSC (H) y HPTSC* (H*) ligands and their complexes. Data are expressed as mean ± standard deviation (n=9). Significant differences ($p<0.05$) among the treatments are expressed in Roman (HT-29) and Greek letters (SW-480) and between cell lines with asterisk (*).

Figure 2. TRX concentration (ng/mL) of HT-29 and SW-480 treated with the HPTSC (H) y HPTSC* (H*) ligands and their complexes. Data are expressed as mean ± standard deviation (n=9). Significant differences ($p<0.05$) among the treatments are expressed in Roman (HT-29) and Greek letters (SW-480) and between cell lines with asterisk (*).

Figure 3. GSH/GSSG ratio of HT-29 and SW-480 treated with the HPTSC (H) y HPTSC* (H*) ligands and their complexes. Data are expressed as mean ± standard deviation (n=9). Significant differences ($p<0.05$) among the treatments are expressed in Roman (HT-29) and Greek letters (SW-480) and between cell lines with asterisk (*).

Figure 4. Carbonyl groups (CGs mmol/mg prot) of HT-29 and SW-480 treated with the

HPTSC (H) y HPTSC* (H*) ligands and their complexes. Data are expressed as mean ± standard deviation (n=9). Significant differences ($p<0.05$) among the treatments are expressed in roman (HT-29) and greek letters (SW-480) and between cell lines with asterisk (*).

Figure 5. MDA concentration (µmol) of HT-29 and SW-480 treated with the HPTSC (H) y HPTSC* (H*) ligands and their complexes. Data are expressed as mean ± standard deviation (n=9). Significant differences ($p<0.05$) among the treatments are expressed in Roman (HT-29) and Greek letters (SW-480) and between cell lines with asterisk (*).

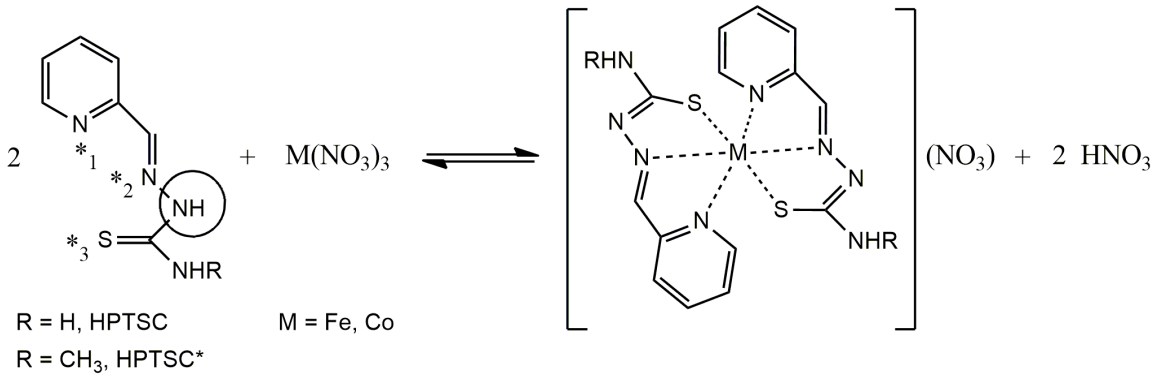

Scheme 1.

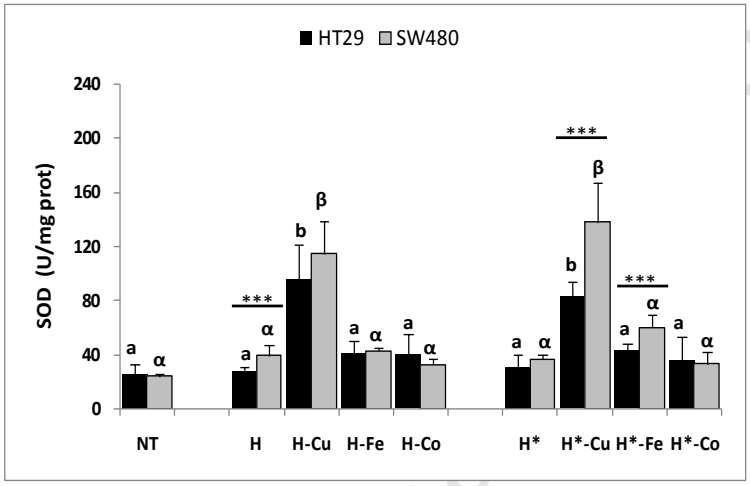

Figure 1.

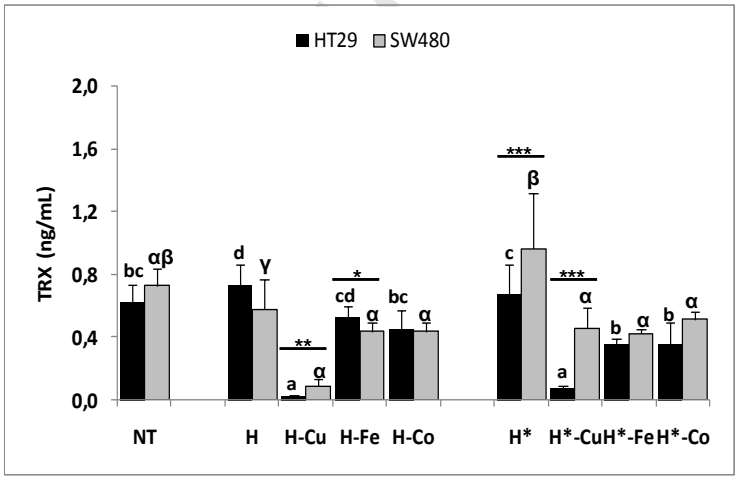

Figure 2.

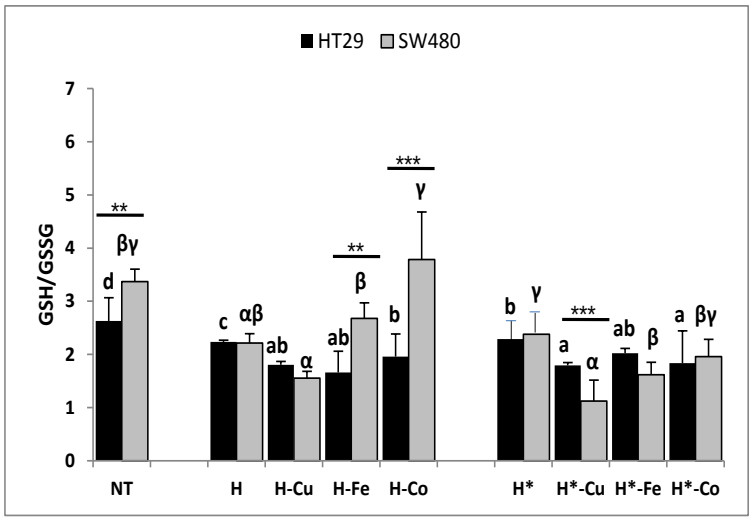

Figure 3.

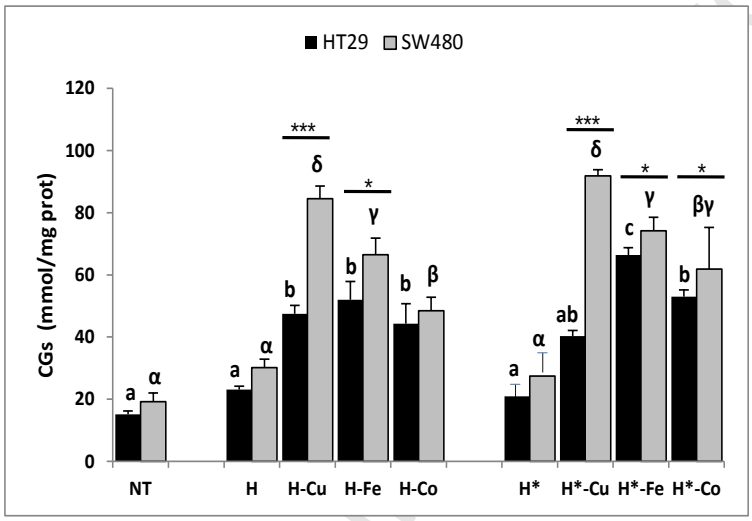

Figure 4.

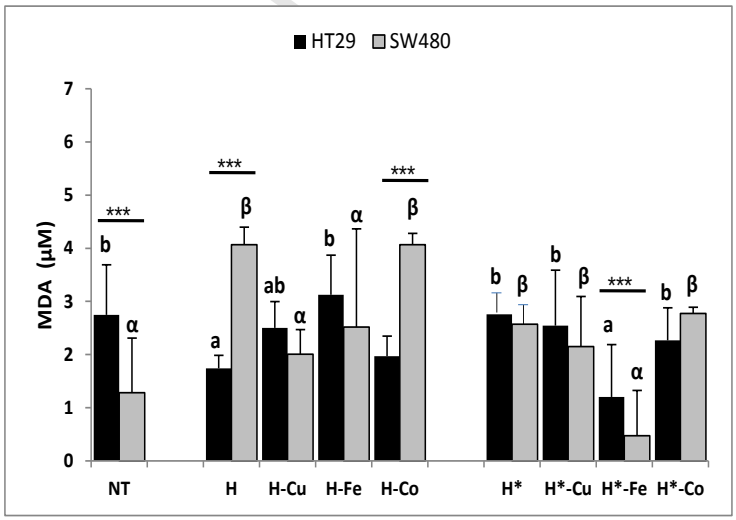

Figure 5.

Table 1. IC50 (µM) of the HPTSC and HPTSC* ligands, their coordination compounds and oxaliplatin, against cancer cells (HT-29 and SW-480) and a normal cell line (CCD-112).

IC50 (µM)							
	HT-29	**SW-480**	**CCD-112**		**HT-29**	**SW-480**	**CCD-112**
HPTSC	49.8±1.03^{d}	29.4±1.16$^{\gamma}$	61.9±0.79 *	**HPTSC***	73,89±2.18^{e}	27.65±1.1$^{\gamma}$ **	79.2±3.12
HPTSC-Cu	5.49±0.20^{a}	5.48±0.79$^{\alpha}$	64.8±5.13 ***	**HPTSC*-Cu**	3.70± 0.23^{a}	3.67±0.14$^{\alpha}$	48.7±4.5 ***
HPTSC-Fe	40.12±2.06^{c}	28.44±1.22$^{\gamma}$	71.8±5.37 **	**HPTSC*-Fe**	12.09±1.07^{b}	19.11±0.95$^{\beta}$	72.9±1.06 ***
HPTSC-Co	32.85±1.54^{c}	34.45±2.06$^{\gamma}$	100±13.9 ***	**HPTSC*-Co**	14.24±0.91^{b}	26.94±1.12$^{\gamma}$	101±5.4 ***
Oxaliplatin	183±25.3 ***	95.44±4.53	118±1.1				

Data are expressed as mean ± standard deviation (n=9, except for oxaliplatin where n = 6). Significant differences ($p<0.05$) among the treatments are expressed in Roman (HT-29) and Greek letters (SW-480) and between cell lines with asterisk (*).

Table 2. 8OH-2dG/2dG ratio, Caspase 3 concentration (µmol), Caspase 9 concentration (µmol) and free histones concentration (µmol) of HT-29 and SW-480 treated with the HPTSC (H) y HPTSC* (H*) ligands and their metal complexes.

	8OH-2dG/2dG		Caspase 3		Caspase 9		Free Histones	
	HT-29	SW-480	HT-29	SW-480	HT-29	SW-480	HT-29	SW-480
NT	0.49±0.09^{a}	0.62±0.23$^{\alpha\beta}$	0.47±0.17^{a}	0.47±0.13$^{\alpha}$	11.53±3.95^{ab}	9.03±1.06$^{\alpha}$	0.35±0.0 1^{a}	0.14±0.01$^{\alpha}$
HPTSC	0.96±0.16^{a}	0.88±0.09$^{\beta}$	3.54±0.54^{bc}	2.77±0.98$^{\beta}$	10.51±1.52^{ab}	10.90±3.85$^{\alpha}$	0.48±0.01^{a}	0.47±0.01$^{\alpha}$
HPTSC-Cu^{II}	2.71±0.61^{c} ***	1.34±0.17$^{\gamma}$	6.46±1.53^{d} *	12.33±5.82$^{\delta}$	26.17±5.78^{c} *	63.80±26.00$^{\delta}$	6,26±0,45^{c} **	8,96±0.65$^{\delta}$
HPTSC-Fe^{III}	0.48±0.09^{a} *	0.25±0.05$^{\alpha}$	3.88±0.07^{c}	4.07±0.36$^{\beta\gamma}$	13.36±1.92^{b}	14.74±1.32$^{\alpha\beta}$	1.10±0.02^{b}	0.98±0.02$^{\beta}$
HPTSC-Co^{III}	0.64±0.2^{a} *	0.32±0.11$^{\alpha}$	2.23±0.48^{b}	2.75±0.13$^{\alpha}$	11.23±2.36^{ab}	15.55±0.71$^{\alpha\beta}$	0.87±0.1^{ab}	0.37±0.01$^{\alpha}$
HPTSC*	0.81±0.16^{a}	0.52±0.21$^{\alpha\beta}$	2.84±0.27^{bc}	3.92±0.90$^{\beta\gamma}$	7.32±0.61^{a}	12.13±2.35$^{\alpha\beta}$	0.82±0.02^{ab}	1.28±0.02$^{\beta}$
HPTSC*-Cu^{II}	2.18±0.66^{b}	2.12±0.14$^{\delta}$	5.91±1.23^{d} *	10.81±4.53$^{\delta}$	24.05±4.69^{c} *	45.27±18.88$^{\gamma}$	6.70±0.52^{c} *	7.94±0.33$^{\gamma}$
HPTSC*-Fe^{III}	0.67±0.09^{a}	0.60±0.17$^{\alpha\beta}$	3.47±0.22^{bc}	4.69±0.81$^{\gamma}$	11.56±0.11^{ab}	22.25±3.88$^{\beta}$	1.11±0.06^{b}	1.04±0.01$^{\beta}$
HPTSC*-Co^{III}	0.58±0.07^{a}	0.74±0.08$^{\alpha\beta}$	2.32±0.98^{b}	2.03±0.18$^{\beta}$	10.96±4.59^{ab}	10.65±1.13$^{\alpha\beta}$	0.96±0.02^{b} *	0.35±0.01$^{\alpha}$

Data are expressed as mean ± standard deviation (n=9 or n=6). Significant differences ($p<0.05$) among the treatments are expressed in Roman (HT-29) and Greek letters (SW-480) and between cell lines with asterisk (*).

Thiosemicarbazone-metal complexes exhibiting cytotoxicity in colon cancer cell lines through oxidative stress

Raquel Alcaraz[a*], Pilar Muñiz[b*], Mónica Cavia[b], Óscar Palacios[c], Katia G. Samper[c], Rubén Gil-García[d], Alondra Jiménez-Pérez [d], Javier García-Tojal[d], Carlos García-Girón[e]

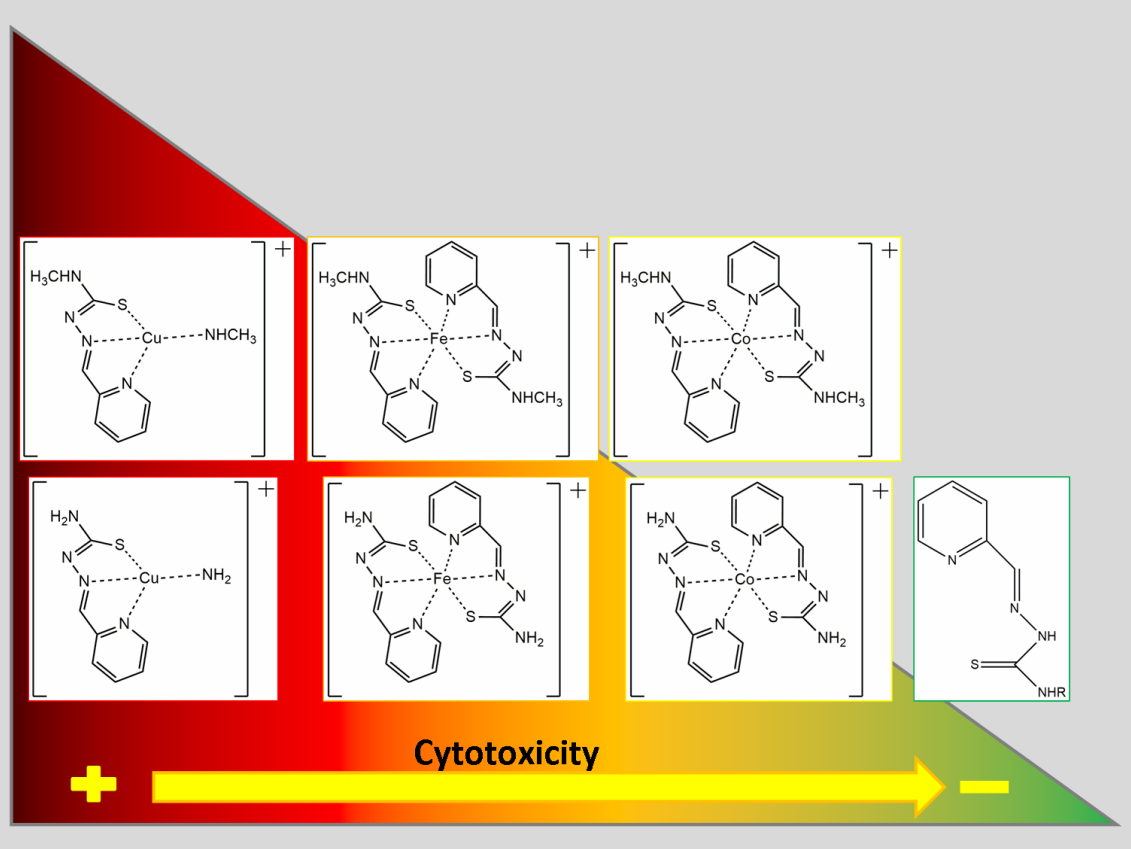

Synopsis. Cytotoxicity ranking on colon cancer cell lines (HT-29 and SW480) with free and metal coordinated thiosemicarbazones. These compounds cause changes in oxidative stress levels in several metabolic points leading to cell death.

Graphical abstract

Thiosemicarbazone-metal complexes exhibiting cytotoxicity in colon cancer cell lines through oxidative stress

Raquel Alcaraz[a*], Pilar Muñiz[b*], Mónica Cavia[b], Óscar Palacios[c], Katia G. Samper[c], Rubén Gil-García[d], Alondra Jiménez-Pérez [d], Javier García-Tojal[d], Carlos García-Girón[e]

Highlights

- Cytotoxicity increases significantly when thiosemicarbazone ligands link metal ions.
- Complexes formed by thiosemicarbazones and Cu(II) have the most proapoptotic activity.
- The methylated Cu(II)-derivative acts in DNA in a prooxidant way and induces apoptosis.